CHEMISTRY OF MATERIALS
Article

Chem. Mater. **2009,** *21,* 2789–2797 2789
DOI:10.1021/cm900383c

Metal-Free Phthalocyanines Bearing Eight Alkylsulfonyl Substituents: Design, Synthesis, Electronic Structure, and Mesomorphism of New Electron-Deficient Mesogens

Benoît Tylleman,[†] Gabin Gbabode,[†] Claire Amato,[†] Claudine Buess-Herman,[‡] Vincent Lemaur,[§] Jérôme Cornil,[§] Rafael Gómez Aspe,[‖] Yves Henri Geerts,*[,†] and Sergey Sergeyev*[,†]

[†]*Laboratory of Polymer Chemistry, Faculté des Sciences, Université Libre de Bruxelles (ULB), CP 206/1, Boulevard du Triomphe, 1050 Bruxelles, Belgium,* [‡]*Laboratory of Analytical and Interface Chemistry, Faculté des Sciences, Université Libre de Bruxelles (ULB), CP 255, Boulevard du Triomphe, 1050 Bruxelles, Belgium,* [§]*Laboratory for Chemistry of Novel Materials, University of Mons-Hainaut, Place du Parc 20, 7000 Mons, Belgium, and* [‖]*Department of Organic Chemistry, Universidad Complutense de Madrid, Avda. Complutense, 28040 Madrid, Spain*

Received February 10, 2009. Revised Manuscript Received May 13, 2009

This paper describes the synthesis and physicochemical characterization of novel metal-free phthalocyanines **Pc(SO$_2$R)$_8$**, bearing eight peripheral alkylsulfonyl substituents. The key synthetic step is the efficient eightfold oxidation of sulfanyl (SR) into sulfonyl (SO$_2$R) functions in the precursor **Pc(SR)$_8$**. Quantum-chemical calculations show a considerable stabilization of the HOMO and LUMO levels of **Pc(SO$_2$R)$_8$** as a result of the presence of the strongly electron-withdrawing groups, while the HOMO−LUMO gap remains nearly unaffected. The redox behavior and electronic spectra of **Pc(SO$_2$R)$_8$** were investigated by cyclic voltammetry and electronic absorption spectroscopy, respectively, to confirm the theoretical predictions. Particularly noteworthy is the first reduction potential of −0.14 V vs the saturated calomel electrode (SCE), which falls within the empirically established air-stability window for n-type semiconductors. Supramolecular structures of mesophases of **Pc(SO$_2$R)$_8$** and their synthetic precursors **Pc(SR)$_8$** were studied in detail with the aid of powder X-ray diffraction in combination with differential scanning calorimetry and polarized light optical microscopy. As it was demonstrated earlier for many different discotic mesogens, installation of either linear or swallow-tail branched peripheral alkyl substituents plays an important role in the formation of mesophases. However, an unusual behavior was found for the **Pc(SO$_2$R)$_8$** series: swallow-tail alkyl chains resulted in higher order in columnar mesophases compared to the linear analogues.

Introduction

Discotic (disk-like) molecules that typically comprise a rigid aromatic core decorated with flexible peripheral chains have been attracting a growing interest because of their fundamental importance for the study of charge and energy transport.[1−4] In addition, the ability of discotic molecules to self-assemble in columnar superstructures together with their capacity to self-heal structural defects in liquid crystalline (LC) columnar mesophases provide considerable potential for their application in organic electronics.[3,5−7] While the majority of disk-like mesogens are electron-rich molecules,[3] various electron-poor discotic mesogens are also known (for selected examples, see refs 8−16 and references cited therein).

---

*Corresponding authors. E-mail: ygeerts@ulb.ac.be (Y.H.G.); sserguee@ulb.ac.be (S.S.).

(1) Adam, D.; Schuhmacher, P.; Simmerer, J.; Haussling, L.; Siemensmeyer, K.; Etzbach, K. H.; Ringsdorf, H.; Haarer, D. *Nature* **1994**, *371*, 141.
(2) Lemaur, V.; da Silva Filho, D. A.; Coropceanu, V.; Lehmann, M.; Geerts, Y.; Piris, J.; Debije, M. G.; van de Craats, A. M.; Senthilkumar, K.; Siebbeles, L. D. A.; Warman, J. M.; Bredas, J.-L.; Cornil, J. *J. Am. Chem. Soc.* **2004**, *126*, 3271.
(3) Sergeyev, S.; Pisula, W.; Geerts, Y. H. *Chem. Soc. Rev.* **2007**, *36*, 1902.
(4) Laschat, S.; Baro, A.; Steinke, N.; Giesselmann, F.; Haegele, C.; Scalia, G.; Judele, R.; Kapatsina, E.; Sauer, S.; Schreivogel, A.; Tosoni, M. *Angew. Chem., Int. Ed.* **2007**, *46*, 4832.
(5) Kumar, S. *Chem. Soc. Rev.* **2006**, *35*, 83.
(6) Watson, M. D.; Fechtenkötter, A.; Müllen, K. *Chem. Rev.* **2001**, *101*, 1267.
(7) Wu, J.; Pisula, W.; Müllen, K. *Chem. Rev.* **2007**, *107*, 718.
(8) Ohta, K.; Hasebe, H.; Ema, H.; Fujimoto, T.; Yamamoto, I. *J. Chem. Soc., Chem. Commun.* **1989**, 1610.
(9) Ohta, K.; Watanabe, T.; Fujimoto, T.; Yamamoto, I. *J. Chem. Soc., Chem. Commun.* **1989**, 1611.
(10) Nishida, J.; Naraso; Murai, S.; Fujiwara, E.; Tada, H.; Tomura, M.; Yamashita, Y. *Org. Lett.* **2004**, *6*, 2007.
(11) Lehmann, M.; Kestemont, G.; Aspe, R. G.; Buess-Herman, C.; Koch, M. H. J.; Debije, M. G.; Piris, J.; de Haas, M. P.; Warman, J. M.; Watson, M. D.; Lemaur, V.; Cornil, J.; Geerts, Y. H.; Gearba, R.; Ivanov, D. A. *Chem.—Eur. J.* **2005**, *11*, 3349.
(12) Foster, E. J.; Jones, R. B.; Lavigueur, C.; Williams, V. E. *J. Am. Chem. Soc.* **2006**, *128*, 8569.
(13) Nolde, F.; Pisula, W.; Müller, S.; Kohl, C.; Müllen, K. *Chem. Mater.* **2006**, *18*, 3715.
(14) Saidi-Besbes, S.; Grelet, E.; Bock, H. *Angew. Chem., Int. Ed.* **2006**, *45*, 1783.
(15) Cho, J.-Y.; Domercq, B.; Jones, S. C.; Yu, J.; Zhang, X.; An, Z.; Bishop, M.; Barlow, S.; Marder, S. R.; Kippelen, B. *J. Mater. Chem.* **2007**, *17*, 2642.
(16) Bisoyi, H. K.; Kumar, S. *New J. Chem.* **2008**, *32*, 1974.

The general interest in electron-deficient π-conjugated molecules is triggered by the need to develop air-stable, high mobility n-type (electron transporting) organic semiconductors, which would complement currently well-developed high performance p-type (hole transporting) semiconductors. The availability of air-stable n- and p-type semiconductors will open new perspectives for the design of complementary p-n circuits compatible with high throughput solution-based manufacturing methods and thus will allow costly vacuum-based fabrication and device encapsulation to be avoided.[17-20]

Phthalocyanines have found a number of industrial applications as dyes and pigments due to their bright blue or green colors combined with extraordinary thermal and photochemical stability.[21] They have also been investigated for their potential use in other fields, including catalysis, chemical sensors, nonlinear optical materials, electrophotography, and photodynamic therapy.[22-24] Phthalocyanines bearing flexible peripheral substituents represent a typical example of discotic mesogens. They have been widely studied for applications in electronic devices and have demonstrated very efficient charge transport.[25] Combination of charge transport capacity with very strong absorption of visible light makes phthalocyanines promising candidates for photovoltaic applications. While there are many examples of mesogenic phthalocyanines bearing electron-donating substituents, phthalocyanines with electron-withdrawing substituents are rather scarcely represented across the chemical literature. In addition to general interest in electron-poor phthalocyanines as n-type semiconductors for p-n circuitry, our particular interest in liquid crystalline, solution-processable electron-deficient phthalocyanines originates from the perspective of their application as acceptor components in bulk-heterojunction photovoltaic cells.

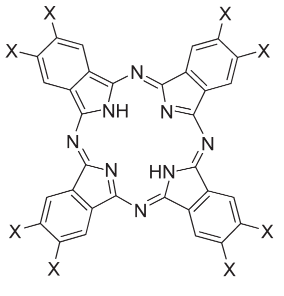

PcH_8: X = H
$Pc(SO_2Me)_8$: X = SO_2Me
$Pc(COOMe)_8$: X = COOMe
$Ps(SMe)_8$: X = SMe

Figure 1. Structures of phthalocyanines involved in the computational study.

Table 1. Calculated Energies of the Frontier Orbitals and of the Two Lowest Optical Transitions S_1, S_2 (in eV) of PcH_8, $Pc(COOR)_8$, $Pc(SO_2R)_8$, and $Pc(SR)_8$[a]

parameter	PcH_8	$Pc(COOR)_8$	$Pc(SO_2R)_8$	$Pc(SR)_8$
LUMO[b]	−1.61	−2.35	−3.07	−1.76
HOMO[b]	−5.53	−6.20	−6.97	−5.67
S_1[b]	1.60	1.57	1.67	1.62
S_2[b]	1.74	1.71	1.80	1.76
E_{1red} found[c]		−0.45	−0.14	−0.88
λ_1 found[c]		1.76	1.76	1.69
λ_2 found[c]		1.86	1.86	1.76

[a] The experimental values of the first reduction potential E_{1red} ($= (Ep_{c1} + Ep_{a1})/2$) and absorption maxima of the Q-bands λ_1, λ_2 (in eV, from cyclic voltammetry and UV-vis spectroscopy, respectively, see text) are also included. [b] R = Me. [c] R = $C_{12}H_{25}$.

Recently, we have reported[26-28] the synthesis, mesophase engineering, and physicochemical characterization of octaester derivatives of phthalocyanines (**$Pc(COOR)_8$**, Figure 1). A joint experimental and theoretical study has shown considerable stabilization of the LUMO level caused by the eight electron-withdrawing ester groups. Here, we describe the synthesis and study of a novel family of electron-deficient phthalocyanine mesogens, octasulfones **1** (= **$Pc(SO_2R)_8$**), designed with the aim of further increasing the electron affinity of phthalocyanine core.

Results and Discussion

Design. Our design of new electron-deficient phthalocyanines is based on a very simple initial entry. An alkylsulfone (SO_2R) is a much stronger electron acceptor compared to an alkyl ester (COOR), as evidenced by values of Hammet constants obtained from the dissociation of substituted benzoic acids: σ_{para} and σ_{meta} are 0.73 and 0.64 for SO_2R and 0.44 and 0.35 for COOR.[29]

We have also computed electronic and optical properties of the octasulfone **$Pc(SO_2Me)_8$** on the basis of the optimized geometry (see Supporting Information). Calculations were performed at the semiempirical Hartree–Fock level with the ZINDO/S method (intermediate neglect of differential overlap) as developed and parametrized by Ridley and Zerner[30] coupled to a single configuration scheme (SCI) including all $\pi-\pi^*$ transitions. The energies of the frontier electronic levels of the octasulfone **$Pc(SO_2Me)_8$** are summarized in Table 1; the corresponding values for the unsubstituted phthalocyanine **PcH_8**, octaester **$Pc(COOMe)_8$**, and octasulfide **$Pc(SMe)_8$** are

---

(17) Jones, B. A.; Facchetti, A.; Wasielewski, M. R.; Marks, T. J. *J. Am. Chem. Soc.* **2007**, *129*, 15259.
(18) Klauk, H.; Zschieschang, U.; Pflaum, J.; Halik, M. *Nature* **2007**, *445*, 745.
(19) De Vusser, S.; Steudel, S.; Myny, K.; Genoe, J.; Heremans, P. *Appl. Phys. Lett.* **2006**, *88*, 162116.
(20) Jung, T.; Yoo, B.; Wang, L.; Dodabalapur, A.; Jones, B. A.; Facchetti, A.; Wasielewski, M. R.; Marks, T. J. *Appl. Phys. Lett.* **2006**, *88*, 183102.
(21) Gregory, P. *J. Porphyrins Phthalocyanines* **2000**, *4*, 432.
(22) McKeown, N. B. Phthalocyanine Materials: Synthesis, Structure and Function; University Press: Cambridge, 1998; p 194.
(23) Ali, H.; Van Lier, J. E. *Chem. Rev.* **1999**, *99*, 2379.
(24) de la Torre, G.; Claessens, C. G.; Torres, T. *Chem. Commun.* **2007**, 2000.
(25) Iino, H.; Hanna, J.; Bushby, R. J.; Movaghar, B.; Whitaker, B. J.; Cook, M. J. *Appl. Phys. Lett.* **2005**, *87*, 132102.
(26) Sergeyev, S.; Pouzet, E.; Debever, O.; Levin, J.; Gierschner, J.; Cornil, J.; Gomez-Aspe, R.; Geerts, Y. H. *J. Mater. Chem.* **2007**, *17*, 1777.
(27) Sergeyev, S.; Debever, O.; Pouzet, E.; Geerts, Y. H. *J. Mater. Chem.* **2007**, *17*, 3002.
(28) Tylleman, B.; Gomez-Aspe, R.; Gbabode, G.; Geerts, Y. H.; Sergeyev, S. *Tetrahedron* **2008**, *64*, 4155.
(29) March, J. Advanced Organic Chemistry; Wiley and Sons: New York, 1985; p 242.
(30) Ridley, J.; Zerner, M. *Theor. Chim. Acta* **1973**, *32*, 111.

Scheme 1. Synthesis of the Phthalocyanines 1a−c[a]

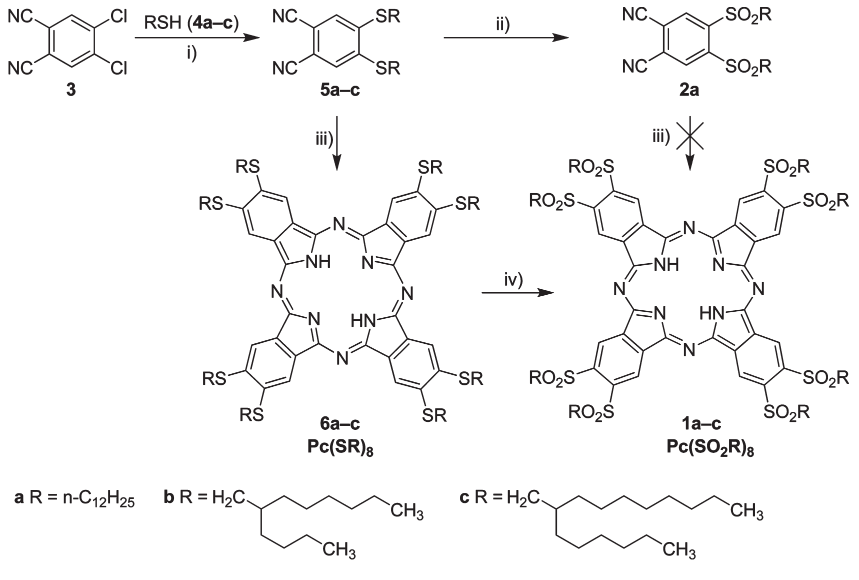

[a] (i) K_2CO_3, DMSO, 100°C; (ii) H_2O_2, AcOH, reflux; (iii) n-$C_5H_{11}OLi/n$-$C_5H_{11}OH$, reflux; and (iv) m-CPBA, CH_2Cl_2, rt.

given for comparison.[26] As expected, the strongly electron withdrawing sulfonyl groups decrease significantly the energy of all electronic levels of **Pc(SO$_2$Me)$_8$**, by approximately 1.5 eV compared to the unsubstituted phthalocyanine and by approximately 0.8 eV compared to **Pc(COOMe)$_8$** bearing moderately electron-withdrawing substituents. On the other hand, the shift of the frontier electronic levels does not change considerably the HOMO−LUMO gap: the energies of the lowest optical transition of the four studied derivatives differ by less than 0.1 eV.

Synthesis. Metal-free octasulfones **1** (=**Pc(SO$_2$R)$_8$**) are, to the best of our knowledge, unknown, although a metalated octakis(alkylsulfonyl)phthalocyanine,[31] as well as several unsymmetrical phthalocyanines[32−35] and subphthalocyanines[36] bearing alkylsulfonyl groups, has been reported earlier by Torres and co-workers. The most general pathway for the synthesis of metal-free phthalocyanines relies on the cyclotetramerization of the suitably substituted *ortho*-dinitriles in the presence of bases.[22,37] We first attempted to prepare **1a** (**Pc(SO$_2$R)$_8$**, R = n-$C_{12}H_{25}$) by the cyclotetramerization of dinitrile **2a** (Scheme 1). The latter was readily prepared from the commercially available 4,5-dichlorophthalonitrile **3** via the twofold nucleophilic substitution with n-$C_{12}H_{25}SH$ (**4a**) according to the published procedure,[38,39] followed by the oxidation of the two sulfide functions in **5a** into sulfone groups with H_2O_2.[33] However, the treatment of dinitrile **2a** with n-$C_5H_{11}OLi/n$-$C_5H_{11}OH$ upon heating produced a complex, inseparable mixture of phthalocyanine derivatives. MALDI-MS data suggest the extensive formation of products resulting from the nucleophilic substitution of sulfonyl groups by alkoxy groups, while no **1a** was detected (see Supporting Information). The nucleophilic substitution in a rather electron-deficient aromatic ring proceeds easily and renders this method of the synthesis of **1a** unfeasible.

In the synthesis of a metalated octakis(alkylsulfonyl) phthalocyanine, Torres and co-workers circumvented this problem via the conversion of the starting dinitrile into the corresponding diiminoisoindoline intermediate upon the action of NH_3 and MeONa in MeOH at 0 °C.[31] Although the nucleophilic substitution by the attack of the methylate anion was indeed observed even in these mild conditions, the diiminoisoindoline intermediate was isolated and then transformed into the corresponding Pd-phthalocyanine, however, in rather modest total yield.

We have therefore developed an alternative three-step synthesis of octasulfones **1** (=**Pc(SO$_2$R)$_8$**), which relies on the eightfold oxidation of the precursors **6** (= **Pc(SR)$_8$**) as a key step. Synthesis of octasuflide **6a** (R = n-$C_{12}H_{25}$) from dinitrile **5a** was reported earlier.[38,40] It should be noted that condensation with n-$C_5H_{11}OLi/n$-$C_5H_{11}OH$ produced better yield of **6a** (57%) than a previously reported procedure with DBU (1,8-diazabicyclo[5.4.0]undec-7-ene) as a base.[38,40] In the crucial step, octasulfone **1a** was prepared

---

(31) De la Escosura, A.; Martínez-Díaz, M. V.; Guldi, D. M.; Torres, T. *J. Am. Chem. Soc.* **2006**, *128*, 4112.

(32) De la Torre, G.; Martinez-Diaz, M. V.; Ashton, P. R.; Torres, T. *J. Org. Chem.* **1998**, *63*, 8888.

(33) Maya, E. M.; Garcia, C.; Garcia-Frutos, E. M.; Vazquez, P.; Torres, T. *J. Org. Chem.* **2000**, *65*, 2733.

(34) De La Escosura, A.; Martinez-Diaz, M. V.; Thordarson, P.; Rowan, A. E.; Nolte, R. J. M.; Torres, T. *J. Am. Chem. Soc.* **2003**, *125*, 12300.

(35) de la Escosura, A.; Martinez-Diaz, M. V.; Barbera, J.; Torres, T. *J. Org. Chem.* **2008**, *73*, 1475.

(36) del Rey, B.; Keller, U.; Torres, T.; Rojo, G.; Agulló-López, F.; Nonell, S.; Martí, C.; Brasselet, S.; Ledoux, I.; Zyss, J. *J. Am. Chem. Soc.* **1998**, *120*, 12808.

(37) Tant, J.; Geerts, Y. H.; Lehmann, M.; de Cupere, V.; Zucchi, G.; Laursen, B. W.; Bjornholm, T.; Lemaur, V.; Marcq, V.; Burquel, A.; Hennebicq, E.; Gardebien, F.; Viville, P.; Beljonne, D.; Lazzaroni, R.; Cornil, J. *J. Phys. Chem. B* **2005**, *109*, 20315.

(38) Ban, K. Z.; Nishizawa, K.; Ohta, K.; Shirai, H. *J. Mater. Chem.* **2000**, *10*, 1083.

(39) Ban, K.; Nishizawa, K.; Ohta, K.; de Craats, A. M. V.; Warman, J. M.; Yamamoto, I.; Shirai, H. *J. Mater. Chem.* **2001**, *11*, 321.

(40) Lux, A.; Rozenberg, G. G.; Petritsch, K.; Moratti, S. C.; Holmes, A. B.; Friend, R. H. *Synth. Met.* **1999**, *102*, 1527.

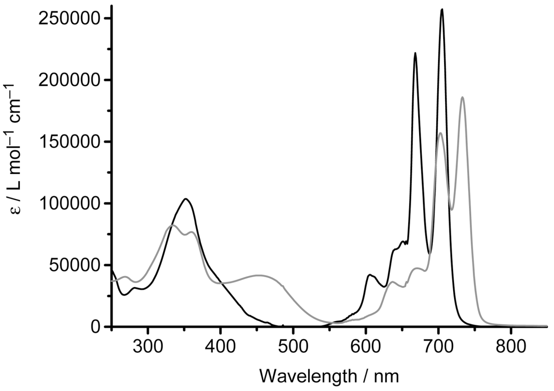

Figure 2. UV−vis absorption spectra of **1c** (black line) and **6c** (gray line) in CH_2Cl_2.

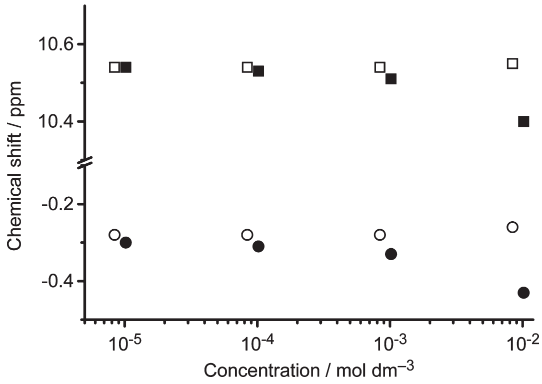

Figure 3. Concentration-dependent ^{1}H chemical shifts in **1a**,**b** in $CDCl_3$. □, ■ = aromatic H; ●, ○ = NH; solid symbols = **1a**, open symbols = **1b**.

by the 8-fold oxidation of **6a** with *m*-chloroperbenzoic acid (*m*-CPBA) under exclusion of light.[41]

Two octasulfones **1b**,**c** bearing branched, swallow-tail alkyl chains (envisaged for the modification of thermotropic properties, see below) were prepared by the same method. The necessary thiols **4b**,**c** were easily synthesized in two steps from the corresponding commercially available alcohols, according to the known general method (see Supporting Information for experimental details and analytical data).[42,43]

All phthalocyanines **1a**−**c** are well soluble in common organic solvents and were readily purified by column chromatography on SiO_2. They were characterized by ^{1}H and ^{13}C NMR spectroscopy, and by IR, UV−vis, and MALDI MS (see Experimental Section for analytical data). The UV−visible absorption spectra of **1a**−**c** in CH_2Cl_2 are nearly identical and feature a double intense low-frequency absorption band (termed Q-band) due to the quasi-degeneracy of the lowest excited state of a D_{2h}-symmetrical molecule (cf. single Q-band due to the degeneracy in D_{4h}-symmetrical metalated phthalocyanines).[22,28]

Compared to **6a**−**c** (= $\mathbf{Pc(SR)_8}$), a hypsochromic shift of the double Q-band (0.07 and 0.10 eV) is observed for **1a**−**c** (= $\mathbf{Pc(SO_2R)_8}$), see Figure 2. This is consistent with the slight increase of the transition energy calculated when going from $\mathbf{Pc(SR)_8}$ to $\mathbf{Pc(SO_2R)_8}$. On the other hand, the absorption spectra of octasulfones $\mathbf{Pc(SO_2R)_8}$ and octaesters $\mathbf{Pc(COOR)_8}$ are merely identical, while calculations (in the gas phase) predict a decrease of the transition energy for $\mathbf{Pc(COOR)_8}$ by approximately 0.1 eV vs $\mathbf{Pc(SO_2R)_8}$. In general, both the experimental and the theoretical data show that the absorption spectra of all phthalocyanines reported here are only slightly affected by the electronic nature of substituents.

On the NMR time scale, the exchange of protons between the inner nitrogen atoms of the phthalocyanine core is fast, and ^{1}H NMR spectra reflect the pseudo D_{4h}-symmetry of the molecule for $\mathbf{Pc(SO_2R)_8}$ and $\mathbf{Pc(SR)_8}$. Thus, ^{1}H NMR spectra display only one singlet for the aromatic protons. Changing the electronic nature of the eight substituents (from electron-donating RS to the electron-withdrawing RSO_2) results in a considerable downfield shift of this signal (from 9.18 ppm for **6c** to 10.54 ppm for **1c**).

It is well-known that phthalocyanines and other discotic molecules tend to self-aggregate in solution due to efficient π−π interactions.[44,45] This process can easily be monitored by ^{1}H NMR spectroscopy, since the ring current of the aromatic core will induce a change in the chemical shift of the protons of a neighboring molecule. Figure 3 presents the variation of the chemical shifts of the aromatic protons in **1a** and **1b** as a function of concentration in $CDCl_3$. There is virtually no effect of the concentration on the chemical shifts in **1b**, while chemical shifts of both the outer and inner protons of the aromatic core in **1a** show pronounced concentration dependence. This means that the self-aggregation of **1b** is prevented by the steric hindrance of the bulky, branched alkyl chains, while **1a** bearing the linear alkyl substituents self-aggregates. This behavior closely resembles that previously observed by us for phthalocyanines bearing eight ester functions.[26]

Electrochemistry. Redox processes of the three octasubstituted phthalocyanines $\mathbf{Pc(COOR)_8}$, $\mathbf{Pc(SO_2R)_8}$, and $\mathbf{Pc(SR)_8}$ (R = $C_{12}H_{25}$ in all cases) were determined by cyclic voltammetry of 5×10^{-4} M solutions in THF or CH_2Cl_2 containing 0.1 M *n*-Bu_4NPF_6. While poorly resolved voltammograms were obtained in THF, CH_2Cl_2 appears as a solvent of choice for all three compounds, allowing well-resolved quasi-reversible reduction waves.

In general, all studied phthalocyanines display a similar behavior, with multiple reduction waves. Four reversible one-electron reduction waves, typical for phthalocyanine derivatives,[46−48] were observed for $\mathbf{Pc(COOR)_8}$ and $\mathbf{Pc(SO_2R)_8}$. In the case of $\mathbf{Pc(SR)_8}$ two clear reduction

---

(41) Carpino, L. A. *J. Org. Chem.* **1973**, *38*, 2600.
(42) Gueugnot, S.; Alami, M.; Linstrumelle, G.; Mambu, L.; Petit, Y.; Larcheveque, M. *Tetrahedron* **1996**, *52*, 6635.
(43) Schapman, F.; Youssef, B.; About-Jaudet, E.; Bunel, C. *Eur. Polym. J.* **2000**, *36*, 1865.
(44) Wu, J.; Fechtenkoetter, A.; Gauss, J.; Watson, M. D.; Kastler, M.; Fechtenkötter, C.; Wagner, M.; Müllen, K. *J. Am. Chem. Soc.* **2004**, *126*, 11311.
(45) Kastler, M.; Pisula, W.; Wasserfallen, D.; Pakula, T.; Müllen, K. *J. Am. Chem. Soc.* **2005**, *127*, 4286.
(46) Swarts, J. C.; Langner, E. H. G.; Krokeide-Hove, N.; Cook, M. J. *J. Mater. Chem.* **2001**, *11*, 434.
(47) González-Rodríguez, D.; Claessens, C. G.; Torres, T.; Liu, S.; Echegoyen, L.; Vila, N.; Nonell, S. *Chem.—Eur. J.* **2005**, *11*, 3881.
(48) Lever, A. B. P.; Pickens, S. R.; Minor, P. C.; Licoccia, S.; Ramaswamy, B. S.; Magnell, K. *J. Am. Chem. Soc.* **1981**, *103*, 6800.

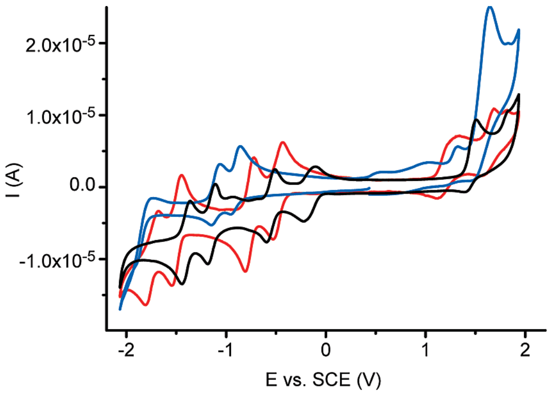

Figure 4. Cyclic voltamogramms of **Pc(COOR)$_8$** (red line), **Pc(SO$_2$R)$_8$** (black line), and **Pc(SR)$_8$** (blue line) in CH_2Cl_2 (R = $C_{12}H_{25}$), scan rate 50 mV s^{-1}.

Table 2. Reduction ($E_{i\text{red}}$) and Oxidation ($E_{i\text{ox}}$) Potentials of Pc(COOR)$_8$, Pc(SO$_2$R)$_8$, and Pc(SR)$_8$ (R = $C_{12}H_{25}$), 5 × 10^{-4} M in CH_2Cl_2, Scan Rate 50 mV s^{-1}

	Pc(CO$_2$R)$_8$	Pc(SR)$_8$	Pc(SO$_2$R)$_8$
$E_{1\text{red}}$	−0.45	−0.88	−0.14
$E_{2\text{red}}$	−0.74	−1.08	−0.53
$E_{3\text{red}}$	−1.47	−1.78	−1.12
$E_{4\text{red}}$	−1.72		−1.38
$E_{1\text{ox}}$	1.13	0.46	1.47
$E_{2\text{ox}}$	1.60	0.96	
$E_{3\text{ox}}$	1.86	1.33	
$E_{4\text{ox}}$		1.60	

signals were observed, likely because further reduction is out of the electrochemical potential window available. All the signals are systematically shifted to more positive values coming from **Pc(SR)$_8$** to **Pc(COOR)$_8$** and then to **Pc(SO$_2$R)$_8$** (see Figure 4 and Table 2). In particular the first reduction potential of **Pc(SO$_2$R)$_8$**, which is of special interest as it provides information about the LUMO level, is shifted by approximately 0.7 and 0.3 V vs **Pc(SR)$_8$** and **Pc(COOR)$_8$**, respectively. The latter observation clearly confirms that stronger electron acceptors do promote a decrease in the LUMO energy, as predicted by the calculations. It should be noted, however, that the gas-phase calculations overestimate the absolute value of the decrease in the LUMO energy versus the electrochemistry results (cf. Table 1 above). Particularly noteworthy is the fact that the first reduction potential of **Pc(SO$_2$R)$_8$** falls within the empirically established air-stability window (between −0.4 and 0 V vs SCE) for n-type semiconductors.[49] This makes octasulfones **Pc(SO$_2$R)$_8$** particularly promising for application as n-type semiconductors.

Structure of Mesophases. As discussed in the Introduction, LC columnar mesophases of discotic materials are particularly interesting for applications based on charge transport. In addition, solution processing followed by thermal annealing is a remarkably facile and potentially cheap method for the fabrication of organic electronic devices. However, a number of conditions should be fulfilled. On the one hand, the materials should form LC phases in a sufficiently broad temperature range, including ambient temperature. On the other hand, processing by thermal annealing requires reasonably low isotropization temperatures in order to avoid thermal decomposition of the semiconductor and/or the plastic substrate. Hence, we investigated in detail the phase structure and thermotropic behavior of octasulfones **1a−c** (= **Pc(SO$_2$R)$_8$**) with the aid of differential scanning calorimetry (DSC), polarized optical microscopy (POM), and powder X-ray diffraction (XRD). For the sake of comparison between the two series of compounds, bearing identical alkyl chains but chemically different linkers between the central core and the peripheral alkyl chains, we investigated also behavior of octasulfides **Pc(SR)$_8$**.

Scheme 2. Thermotropic Behavior of 1a−c^b

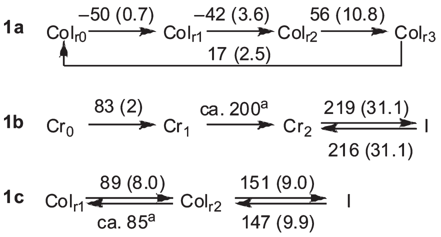

^{a} determined by XRD. ^{b} The temperatures (°C) and enthalpies (in brackets, kJ mol^{-1}) of the phase transitions are determined by DSC from the second heating/cooling cycle, unless stated otherwise, see text. Abbreviations for phases: Cr = crystalline, Col$_h$ = hexagonal columnar, Col$_r$ = rectangular columnar, I = isotropic.

Octasulfide **6a** bearing linear alkyl chains was studied previously: it exhibits various crystalline phases at low temperatures and forms a columnar hexagonal (Col$_h$) LC mesophase with a clearing point at approximately 280 °C.[38,40] As expected,[3,26,50,51] replacement of linear alkyl chains by swallow-tail ones results in considerable decrease of transition temperatures: **6b** forms a Col$_h$ mesophase above −150 °C and melts into isotropic liquid at 56 °C (the enthalpy of this phase transition is too low to be measured by DSC; however, the transition is clearly observable by POM and XRD experiments; cell parameters and peak indexations of the Col$_h$ phase of **6b** are given in the Supporting Information). Further elongation of branched alkyl chains (**6c**) gives a material, which is isotropic in the whole investigated temperature range (above −150 °C).

Octasulfones **1a−c** displayed a rather contrasting and more complex thermotropic behavior (Scheme 2). For **1a** bearing linear alkyl substituents, three endothermic transitions were observed upon heating, suggesting the existence of four different phases. However, on cooling only one exothermic transition was observed. The existence of four different phases was unambiguously confirmed by XRD, with all phases exhibiting two intense reflections in the low angle region (2θ < 5°) and a diffuse halo at high angles (distance of around 4.9 Å) corresponding to the liquid-like arrangement of the linear alkyl chains. In the

---

(49) Wang, Z.; Kim, C.; Facchetti, A.; Marks, T. J. *J. Am. Chem. Soc.* **2007**, *129*, 13362.

(50) Pisula, W.; Tomovic, Z.; El Hamaoui, B.; Watson, M. D.; Pakula, T.; Müllen, K. *Adv. Funct. Mater.* **2005**, *15*, 893.

(51) Pisula, W.; Kastler, M.; Wasserfallen, D.; Mondeshki, M.; Piris, J.; Schnell, I.; Müllen, K. *Chem. Mater.* **2006**, *18*, 3634.

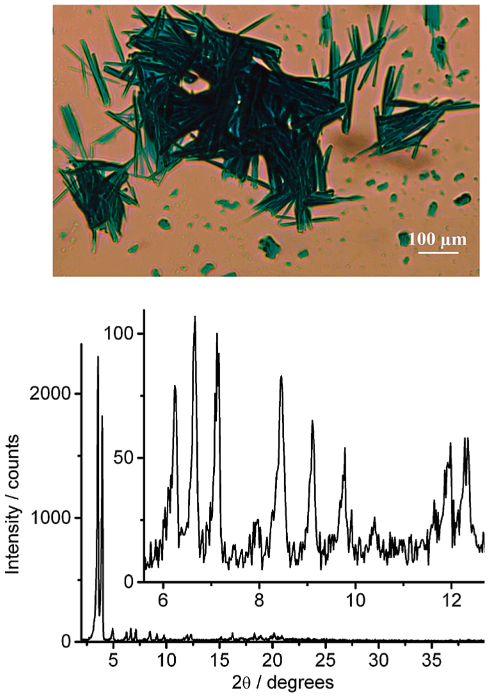

Figure 5. Microphotograph of needle-like crystals of **1b** (Cr_2 phase) at 27 °C after cooling from the isotropic melt (top); XRD pattern of the Cr_2 phase of **1b** measured at room temperature; the inset shows a zoom of the $5.5° < 2\theta < 13°$ region (bottom).

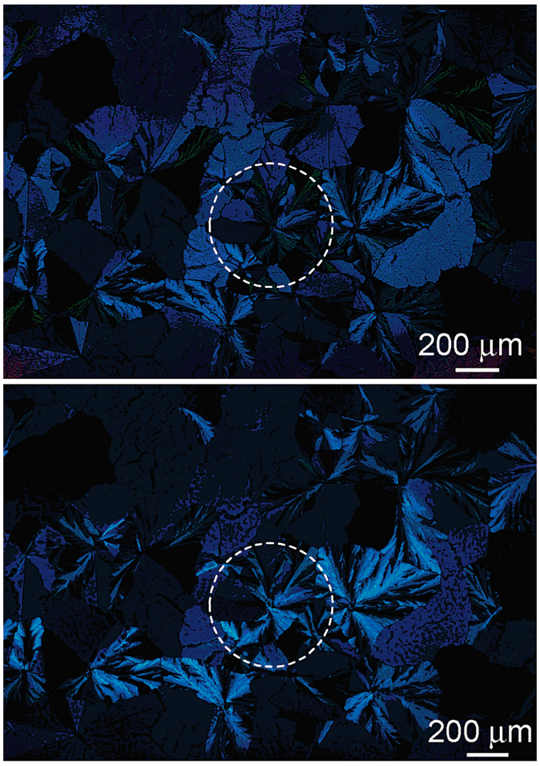

Figure 6. POM images of **1c** at room temperature (top, Col_{r1}) and 115 °C (bottom, Col_{r2}); a part with visible changes in brightness is circled.

case of the highest-temperature phase (measurement at 85 °C), several less intense higher order reflections were detected at $6° < 2\theta < 10°$. All these features are indicative of LC columnar mesophases. However, rather broad reflections evidence poor intercolumnar order (the correlation length of intercolumnar stacking calculated with the Sherrer formula was between four and nine columns for the different mesophases of **1a**).

In the case of **1b** bearing swallow-tail 2-butyloctyl substituents, the first DSC heating revealed, in addition to the isotropization at 219 °C (31 kJ mol^{-1}), an endothermic peak at 83 °C (2 kJ mol^{-1}). Variable-temperature XRD confirmed that the latter is due to the transition between the two crystalline phases (Cr_0/Cr_1) and revealed one more phase transition at approximately 200 °C (Cr_1/Cr_2). However, upon subsequent heating–cooling cycles only isotropization was observed by DSC, and only the Cr_2 phase was observed between room temperature and the melting point by XRD. The XRD pattern of Cr_2 exhibits a number of sharp intense reflections at $2\theta < 25°$, evidencing the 3D crystalline lattice. In addition, no fluid birefringent textures characteristic of LC phases were observed for **1b**. Instead, cooling from the melt gave small needle-like crystals, which remained unchanged during the cooling down to room temperature and the subsequent heating until the melting point (Figure 5). Thus, we observed an unusual case where installing bulky swallow-tail alkyl chains on a discotic core results in the formation of a crystalline phase.

Finally, phthalocyanine **1c** bearing longer 2-hexyldecyl branched chains has an isotropization temperature of 152 °C. Another transition was observed by DSC and XRD only on heating (at 89 °C) and was attributed to a transition between two columnar phases (Col_{r1}/Col_{r2}). In POM experiments, both Col_{r1} and Col_{r2} revealed fluid, birefringent fan-like textures, confirming the LC nature of the two phases. The textures of the two LC phases are very similar, but distinct changes in the brightness of individual features are observed upon Col_{r1}/Col_{r2} transition (Figure 6). From the XRD patterns, the plane group *C*2*mm* has been attributed to Col_{r2} on the basis of the observed reflections,[4] while for Col_{r1} phase plane groups *C*2*mm* and *P*2*gg* are possible. The intercolumnar order is higher in the columnar mesophases of **1c** vs **1a** (correlation length of ca. 40 vs ca. 9 molecules, respectively)

As a summary of the mesophase studies, the decrease of the crystal/LC transition temperatures upon replacing linear alkyl chains by branched ones, which is typical for various structurally different discotic mesogens,[3,26,50,51] does not take place in the $\mathbf{Pc(SO_2R)_8}$ series. Indeed, **1b** bearing branched alkyl chains exhibits a well ordered crystalline phase over a broad temperature range, while the analogue **1a** bearing linear alkyl chains with the same number of carbon atoms forms less ordered columnar mesophases.

Generally, relatively bulky branched alkyl chains reduce the stacking between the flat aromatic cores of discotic molecules due to steric hindrance, thus stabilizing LC mesophases vs crystalline phases and also decreasing isotropization temperatures.[52] For $\mathbf{Pc(SO_2R)_8}$ bearing branched chains, the two-dimensional intercolumnar order is *increased* versus the linear analogues, as evidenced

---

(52) Collard, D. M.; Lillya, C. P. *J. Am. Chem. Soc.* **1991**, *113*, 8577.

by the intercolumnar correlation length values for **1c** vs **1a**. This observation might be explained by the better space filling of the swallow-tail branched alkyl chains, which results in a more compact packing of columnar stacks. Octasulfone **1b** appears as a particularly interesting case: the two-dimensional order of the columnar packing is improved vs the analogue **1a** with linear chains, while the steric hindrance created by branched but comparatively short alkyl chains is relatively small. The combination of these two factors results in a three-dimensional crystalline order. Further elongation of branched chains (**1c**) increases sterical hindrance and produces columnar LC mesophases, which are stable over a broad temperature range.

Similarly to the earlier reported octaesters **Pc-(COOR)$_8$**,[26] octasulfones **1a**–**c** form rectangular rather than hexagonal columnar mesophases. This may originate from the repulsion of the oxygen atoms of relatively bulky COO or SO_2 functions of the neighboring molecules, which introduces a tilt of the molecules with respect to the long columnar axes. For comparison, octasulfides **6a**[38] and **6b** with a smaller linker (i.e., sulfur atom bearing no additional substituents) form Col$_h$ phases, in which disk-like molecules are perpendicular to the long columnar axes.

Finally, it should be noted that phthalocyanines **1b**,**c** and **6b**,**c** with branched chains were prepared starting from the racemic thiols **4b**,**c** and hence represent complex mixtures of diastereoisomers. As was demonstrated earlier,[53] isolation of such materials by chromatography may result in the variation of the stereochemical composition between different fractions, and as a consequence, in the variation of thermotropic properties. Differences in transition temperature between discotic materials prepared from either optically pure or racemic starting materials are also documented.[54] To exclude any discrepancies in thermotropic properties, we aimed to collect during the purification by chromatography all the fractions containing the target phthalocyanines **1b**,**c**. We did not observe any significant variation in the thermotropic properties between different batches of **6b** and **1b**,**c**. It can also be explained by the fact that although 2-butyloctyl (**1b**,**6b**) and 2-hexyldecyl (**1c**,**6c**) groups are formally chiral, they should actually be treated as pseudoachiral since the difference between the two of the substituents at the asymmetric carbon (the two linear alkyls of different length) is very small. Hence, the complex diastereoisomeric mixtures **1b**,**c** and **6b**,**c** behave essentially as they would as individual compounds. This is in perfect agreement with our earlier observations on other mesogenic phthalocyanines bearing swallow-tail branched alkyl chains.[26–28,37]

Conclusion

In summary, we have reported a series of new electron-deficient mesogens, phthalocyanines **Pc(SO$_2$R)$_8$**, designed as air-stable *n*-type (electron transport) semiconductors. Quantum-chemical calculations predict a considerable decrease in the energy of the HOMO and LUMO levels induced by the eight electron-withdrawing sulfone groups. This conclusion is further supported by the electrochemical studies, which show good electron acceptor ability of octasulfones **Pc(SO$_2$R)$_8$**. Particularly noteworthy is the first reduction potential of −0.14 V vs SCE, which falls within the empirically established air-stability window for *n*-type semiconductors. Short synthesis and simple purification allow the preparation of **Pc(SO$_2$R)$_8$** on a multigram scale, which is a prerequisite for a material to find practical applications.

The variation of the peripheral substituents represents an efficient way to adjust the thermotropic properties of these novel discotic mesogens. In particular, a liquid crystalline columnar mesophase between ambient temperature and a reasonably low clearing point (ca. 150 °C) was observed for **1c**. The important prerequisites for the fabrication of *n*-type semiconductor devices by the combination of solution processing and thermal annealing methods are thus fulfilled for the phthalocyanine **1c**. Further objectives include studies of electron transport in the columnar mesophases and the fabrication of devices incorporating these materials.

Experimental Section

Materials and Methods. All chemicals were purchased from Aldrich or Acros and used without further purification unless stated otherwise. Phthalonitrile **5a** was prepared as described previously.[39] Synthesis of thiols **4b**,**c** is described in the Supporting Information. Column chromatography: SiO_2 Kieselgel 60 (Macherey-Nagel, particle size 0.04−0.063 mm). TLC: precoated SiO_2 plates Kieselgel 60F$_{254}$ (Merck). ^{1}H NMR (300 MHz) and ^{13}C NMR (75 MHz) spectra were recorded on a Bruker Avance 300 at 25 °C; chemical shifts (δ) are given in ppm relative to Me$_4$Si (internal standard); coupling constants (J) are given in Hz. MALDI-TOF mass spectra were measured on a Waters QToF Premier, with 1,8-dihydroxy-10*H*-anthracen-9-one (dithranol) or α-cyano-4-hydroxycinnamic acid as a matrix; EI mass spectra were recorded on a Waters AutoSpec 6; m/z with the lowest isotopic mass are reported. UV−vis spectra were recorded on a Hewlett-Packard 8453 spectrophotometer. IR spectra were recorded on a Nicolet 5700 from KBr pellets or from neat substances on NaCl plates. Phase transition temperatures and enthalpies were determined by differential scanning calorimetry on a Perkin-Elmer Diamond DSC, scanning rates between 10 °C min^{-1} and 40 °C min^{-1}; at least four heating−cooling cycles were undertaken for every sample. Optical textures were observed with a polarizing microscope (Nikon Eclipse 80i) equipped with a digital camera (Nikon DS-5M) and a hot stage (Linkam Scientific Instruments CI 94). All samples were prepared on precleaned glass slides.

Powder X-ray diffraction measurements were performed on a Bruker D8 Advance diffractometer using Cu Kα radiation (λ = 1.5418 Å). All samples were prepared on thin precleaned aluminum plates. The material was spread on the aluminum substrate to form a uniform layer (thickness of ca. 0.5 mm) to avoid additional broadening of the diffraction peaks. The sample temperature was controlled within a 0.1 °C accuracy. Diffraction patterns were collected in the scattered angular

---

(53) Kumar, S.; Varshney, S. K. *Angew. Chem., Int. Ed.* **2000**, *39*, 3140.

(54) Fechtenkötter, A.; Tchebotareva, N.; Watson, M.; Müllen, K. *Tetrahedron* **2001**, *57*, 3769.

range between 1.6° and 40° with the angular resolution 0.02° per step and a typical counting time of 10 s per step, using the reflection geometry (θ/θ setup). X-ray diffraction patterns are represented as the scattering intensity versus the angle between the incident and diffracted X-ray beams 2θ (in degrees). The correlation length is determined from the width of the low angle higher intense diffraction peak (intercolumnar distance) using the Sherrer formula: L (Å) = $K\lambda/(\beta \cos \theta)$, where K is a constant ($K = 0.9$), λ is the wavelength of the X-ray radiation (1.5418 Å), β is the full width at half-maximum of the peak expressed in 2θ (radians), and θ is the angular position of the peak. This length is normalized by the interplane distance (given by the position of the diffraction peak using Bragg's law) so that it can be expressed in number of columns.

Cyclic voltammetry experiments were performed with a computer controlled Autolab potentiostat. Measurements were carried out at room temperature in a three-electrode single-compartment cell (10 mL). A glassy carbon, polished by a slurry suspension of alumina on microcloth and washed by Milli-Q water before each experiment, was used as the working electrode. A spiral platinum wire was employed as counter electrode, and an Ag/AgCl/KCl(sat) used as reference electrode was connected to the cell solution via a salt bridge containing a KCl-saturated aqueous solution. The Ag/AgCl electrode was checked against the ferrocene/ferrocinium (Fc/Fc^+) couple ($E°_{Fc/Fc+}$ = 0.425 V vs Ag/AgCl) before and after each experiment. All potentials are reported versus saturated calomel electrode (SCE) ($E°_{Fc/Fc+}$ = 0.405 V vs SCE). Scan rates between 20 and 200 mV s^{-1} were investigated.

All solutions were prepared in freshly distilled anhydrous CH_2Cl_2 or THF containing 0.1 M tetrabutylammonium hexafluorophosphate (n-Bu_4NPF_6, Aldrich), as supporting electrolyte. Before each measurement, oxygen was removed from solutions by 10 min of nitrogen bubbling.

4,5-Bis(2-butyloctylsulfanyl)phthalonitrile, Mixture of (*R*,*R*/*S*,*S*) and *meso*-Diastereoisomers (5b). A solution of 4,5-dichlorophtalonitrile **3** (1.20 mmol, 0.236 g) and (±)-2-butyloctanethiol **4b** (2.88 mmol, 0.583 g) in DMSO (5 mL) was heated to 100 °C, and oven-dry K_2CO_3 (12.0 mmol, 1.656 g) was added in five portions over 30 min. The resulting mixture was stirred at 100 °C for 30 min, allowed to reach room temperature, poured in water (15 mL), and extracted with CH_2Cl_2 (3 × 15 mL). Combined organic layers were dried over $MgSO_4$ and evaporated. The residue was purified by column chromatography (SiO_2, hexane/CH_2Cl_2 1:1) to give **5b** (0.526 g, 83%). Colorless oil. R_f (CH_2Cl_2/hexane, 1:1): 0.23. IR (NaCl): ν (cm^{-1}) = 3080w, 2956s, 2927s, 2856s, 2229s (C≡N), 1564s, 1458s, 1379m, 1346m, 1225m, 1142m, 1315m, 931m, 875w, 737w, 688w; δ_H (300 MHz, in $CDCl_3$, Me_4Si, 25 °C) 7.41 (2H, s, CH_{arom}), 2.97 (4H, d, J = 6.1 Hz, CH_2S), 1.69−1.83 (2H, m, $CHCH_2S$), 1.20−1.54 (32H, m, CH_2), 0.81−0.99 (12H, m, CH_3); δ_C (75 MHz, in $CDCl_3$, Me_4Si, 25 °C) 144.9 (CS), 128.2 (CH_{arom}), 115.7 (CN), 110.9 (*C*CN), 37.7 (CH_2S), 37.1, 33.4, 33.0, 31.8, 29.5, 28.7, 26.5, 22.9, 22.7, 14.09 (CH_3), 14.05 (CH_3). m/z (HR-EI): calcd, 528.3538 ($C_{32}H_{52}N_2S_2$); found, 528.3545 (M^+).

4,5-Bis(2-hexyldecylsulfanyl)phthalonitrile Mixture of (*R*,*R*/*S*,*S*) and *meso*-Diastereoisomers (5c). 5c was prepared similarly to **5a** starting from (±)-2-hexyldecanethiol **4c** (3.50 mmol, 0.904 g). Column chromatography (SiO_2, hexane/CH_2Cl_2 1:1) afforded **5c** (0.841 g, 78%). Colorless oil. R_f (CH_2Cl_2/hexane, 1:1): 0.35. IR (NaCl): ν (cm^{-1})=3079w, 2955s, 2926s, 2870s, 2855s, 2229s (CN), 1564s, 1528w, 1458s, 1378m, 1347m, 1224m, 1142m, 952w, 932m, 876m, 723m, 686w; δ_H (300 MHz, in $CDCl_3$, Me_4Si, 25 °C) 7.41 (2H, s, CH_{arom}), 2.96 (4H, d, J = 6.1 Hz, CH_2S), 1.69−1.83 (2H, m, *CH*CH_2S), 1.18−1.52 (48H, m, CH_2), 0.83−0.98 (12H, m, CH_3); δ_C (75 MHz, in $CDCl_3$, Me_4Si, 25 °C) 144.9 (CS), 128.2 (CH_{arom}), 115.7 (CN), 110.9 (*C*CN), 37.7 (CH_2S), 37.1, 33.4, 31.9, 31.8, 29.8, 29.54, 29.51, 29.3, 26.53, 26.50, 22.68, 22.66, 14.12 (CH_3), 14.09 (CH_3). m/z (HR-EI): calcd, 640.4824 ($C_{40}H_{68}N_2S_2$); found, 640.4815 (M^+).

2,3,9,10,16,17,23,24-Octakis(dodecylsulfanyl)phthalocyanine (6a). A mixture of Li (0.006 g, 0.86 mmol) and dry n-pentanol (3.0 mL) was heated to reflux in Ar until Li is dissolved and then cooled to room temperature. To the resulting solution was added phthalonitrile **5a** (0.264 g, 0.50 mmol), and the mixture was heated to reflux for 15 h, allowed to reach room temperature, and acidified with AcOH to pH 6. Water (5.0 mL) was added, and the dark-green precipitate formed was filtered, redissolved in the minimal amount of CH_2Cl_2, and applied on a dry SiO_2 column. Elution with MeOH removed the residual n-pentanol, and then elution with CH_2Cl_2 afforded 0.152 g (57%) of phthalocyanine **6a**. Dark-green solid. R_f (CH_2Cl_2): 1.00. IR (KBr): ν (cm^{-1}) = 3300w (N—H), 2954m, 2922s, 2850s, 1957m, 1468m, 1421m, 1400m, 1371w, 1327w, 1288w, 1126w, 1074w, 1026m, 937w, 870w, 746m, 721w, 681w, 667m (C—S); δ_H (300 MHz, 2.17×10^{-3} M in $CDCl_3$, Me_4Si, 25 °C) 8.52 (8H, bs, CH_{arom}), 3.45 (16H, t, J = 6.5 Hz, CH_2S), 2.05−2.19 (16H, m, *CH_2*CH_2S), 1.75−1.88 (16H, m, CH_2), 1.15−1.60 (128H, m, CH_2), 0.84 (24H, t, J = 6.8 Hz, CH_3); λ_{max} (CH_2Cl_2)/nm (ε/dm^3 cm^{-1} mol^{-1}) 329 (5.30×10^4), 359 (4.44×10^4), 448 (2.42×10^4), 700 (7.05×10^4), 730 (6.87×10^4); m/z (MALDI) 2115 (M^+).

2,3,9,10,16,17,23,24-Octakis(2-butyloctylsulfanyl)phthalocyanine, Mixture of Diastereoisomers (6b). 6b was prepared similarly to **6a** from **5b** (0.264 g, 0.50 mmol). Yield 42%. Dark-green solid. R_f (CH_2Cl_2): 1.00. IR (KBr): ν (cm^{-1}) = 3292w (N—H), 2990−2780 (broad), 1595m, 1502w, 1458m, 1417m, 1398m, 1377w, 1325w, 1286w, 1126w, 1074m, 1018m, 935m, 752m, 683w, 667w (C—S); δ_H (300 MHz, 9.7×10^{-3} M in $CDCl_3$, Me_4Si, 25 °C) 9.16 (8H, s, CH_{arom}), 3.44 (16H, d, J = 5.7 Hz, CH_2S), 1.91−2.06 (8H, m, *CH*CH_2S), 1.19−1.80 (128H, m, CH_2), 0.96 (24H, t, J = 7.0 Hz, CH_3), 0.82 (24H, t, J = 7.0 Hz, CH_3), −0.87 (2H, bs, NH); δ_C (75 MHz, 0.97×10^{-2} M in $CDCl_3$, Me_4Si, 25 °C) 141.4 (CS), 133.9 (*C*CH_{arom}CS), 121.6 (*CH_{arom}*CS), 39.0, 37.7, 33.6, 33.3, 31.9, 29.8, 29.0, 26.8, 23.1, 22.7, 14.2 (CH_3), 14.1 (CH_3); λ_{max} (CH_2Cl_2)/nm (ε/dm^3 cm^{-1} mol^{-1}) 334 (7.59×10^4), 359 (6.96×10^4), 457 (3.21×10^4), 703 (1.35×10^5), 733 (1.60×10^5). m/z (HR-MALDI): calcd, 2115.4444 ($C_{128}H_{210}N_8S_8$); found 2115.4377 (M^+).

2,3,9,10,16,17,23,24-Octakis(2-hexyldecylsulfanyl)phthalocyanine, Mixture of Diastereoisomers (6c). Prepared similarly to **6a** from **5c** (0.320 g, 0.50 mmol). Yield 49%. Dark-green solid. R_f (CH_2Cl_2): 1.00. IR (KBr): ν (cm^{-1}) 3292w (N—H), 2955s, 2924s, 2870s, 2854s, 1597m, 1501w, 1466m, 1417m, 1399m, 1377m, 1326w, 1286m, 1074m, 1018m, 936m, 752m, 722m, 682m; δ_H (300 MHz, 9.20×10^{-3} M in $CDCl_3$, Me_4Si, 25 °C) 9.18 (8H, bs, CH_{arom}), 3.45 (16H, d, J = 5.1 Hz, CH_2S), 1.93−2.11 (8H, m, *CH*CH_2S), 1.12−1.81 (192H, m, CH_2), 0.82 (24H, t, J = 7.0 Hz, CH_3), 0.76 (24H, t, J = 7.0 Hz, CH_3); δ_C (75 MHz, 9.50×10^{-3} M in $CDCl_3$, Me_4Si, 25 °C) 141.5 (CS), 134.0 (*C*CH_{arom}CS), 121.6 (*CH_{arom}*CS), 39.0, 37.8, 33.6, 32.0, 31.9, 30.1, 29.8, 29.7, 29.4, 26.9, 26.8, 22.7, 22.6, 14.1 (CH_3), 14.0 (CH_3); λ_{max} (CH_2Cl_2)/nm (ε/dm^3 cm^{-1} mol^{-1}) = 335 (7.82×10^4), 360 (7.28×10^4), 451 (3.77×10^4), 703 (1.53×10^5), 733 (1.82×10^5). m/z (HR-MALDI): calcd, 2563.9452 ($C_{160}H_{274}N_8S_8$); found, 2563.9536 (M^+).

2,3,9,10,16,17,23,24-Octakis(dodecylsulfonyl)phthalocyanine (1a). m-Chloroperbenzoic acid (m-CPBA) (0.173 g, ca. 0.77 mmol) was slowly added to a solution of phthalocyanine

6a (0.079 g, 0.04 mmol) in CH_2Cl_2 (7.0 mL) and stirred at room temperature for 16 h in the dark. The reaction mixture was then directly applied on the SiO_2 column; elution with CH_2Cl_2 afforded 0.047 g (53%) of phthalocyanine **1a**. Dark-green solid. R_f (CH_2Cl_2): 0.66. IR (KBr): ν (cm^{-1}) = 3292w (N—H), 3089w, 2954m, 2926s, 2854s, 1502w, 1468w, 1296s (O=S=O asym.), 1146s (O=S=O sym.), 1119m, 1082w, 1016m, 922w, 733w, 667m (C—S); δ_H (300 MHz, 1.02×10^{-4} M in $CDCl_3$, Me_4Si, 25 °C) 10.53 (8H, s, CH_{arom}), 4.00−4.10 (16H, m, CH_2SO_2), 2.08−2.20 (16H, m, $\mathit{CH_2}CH_2SO_2$), 1.14−1.63 (144H, m, CH_2), 0.81 (24H, t, J = 6.8 Hz, CH_3), −0.31 (2H, s, NH); λ_{max} (CH_2Cl_2)/nm (ε/dm^3 cm^{-1} mol^{-1}) 352 (8.18×10^4), 667 (1.87×10^5), 704 (2.17×10^5). m/z (HR-MALDI): calcd, 2394.3528 ($C_{128}H_{210}N_8O_{16}S_8Na$); found, 2394.3545 ($[M + Na]^+$).

2,3,9,10,16,17,23,24-Octakis(2-butyloctylsulfonyl)phthalocyanine, Mixture of Diastereoisomers (1b). 1b was prepared similarly to **1a** from **6b** (0.079 g, 0.04 mmol). Yield 71%. Dark-green solid. R_f (CH_2Cl_2): 0.97. IR (KBr): ν (cm^{-1}) = 3294w (N—H), 3082w, 2956s, 2929s, 2858s, 1468m, 1294s (O=S=O asym.), 1146s (O=S=O sym.), 1117m, 1011m, 922w, 768w, 667w (C—S); δ_H (300 MHz, 0.84×10^{-2} M in $CDCl_3$, Me_4Si, 25 °C) 10.55 (8H, s, CH_{arom}), 3.90−4.05 (16H, m, CH_2S), 2.54−2.66 (8H, m, $\mathit{CH}CH_2S$), 1.18−1.78 (128H, m, CH_2), 0.96 (24H, t, J = 6.8 Hz, CH_3), 0.81 (24H, t, J = 6.7 Hz, CH_3), −0.28 (2H, s, NH); δ_C (75 MHz, 0.84×10^{-2} M in $CDCl_3$, Me_4Si, 25 °C) 143.6 (CSO_2), 139.2 ($\mathit{C}CH_{arom}CSO_2$), 129.2 ($\mathit{CH_{arom}}CSO_2$), 61.7 (CH_2SO_2), 33.5, 33.4, 33.1, 31.8, 29.5, 28.1, 25.9, 22.8, 22.6, 14.08 (CH_3), 14.05 (CH_3); λ_{max} (CH_2Cl_2)/nm (ε/dm^3 cm^{-1} mol^{-1}) 352 (8.99×10^4), 668 (2.05×10^5), 705 (2.34×10^5). m/z (HR-MALDI): calcd, 2394.3528 ($C_{128}H_{210}N_8O_{16}S_8Na$); found, 2394.3567 ($[M + Na]^+$).

2,3,9,10,16,17,23,24-Octakis(2-hexyldecylsulfonyl)phthalocyanine, Mixture of Diastereoisomers (1c). 1c was prepared similarly to **1a** from **6c** (0.102 g, 0.04 mmol). Yield 79%. Dark-green solid. R_f (CH_2Cl_2): 0.96. IR (KBr): ν (cm^{-1}) 3292w (N—H), 3082w, 2955s, 2925s, 2870s, 2854s, 1499w, 1466m, 1419w, 1378w, 1294s (O=S=O asym.), 1144s (O=S=O sym.); δ_H (300 MHz, 3.50×10^{-3} M in $CDCl_3$, Me_4Si, 25 °C) 10.54 (8H, s, CH_{arom}), 3.98 (16H, m, CH_2SO_2), 2.57−2.69 (8H, m, $\mathit{CH}CH_2SO_2$), 1.58−1.79 (16H, m, CH_2), 1.03−1.55 (176H, m, CH_2), 0.68−0.87 (48H, m, CH_3); δ_C (75 MHz, 3.50×10^{-3} M in $CDCl_3$, Me_4Si, 25 °C) 143.7 (CSO_2), 129.2, 61.7, 33.5, 33.4, 31.84, 31.80, 29.9, 29.6, 29.5, 29.3, 26.0, 25.9, 22.64, 22.61, 14.06 (CH_3), 14.03 (CH_3); λ_{max} (CH_2Cl_2)/nm (ε/dm^3 cm^{-1} mol^{-1}) 352 (9.97×10^4), 668 (2.18×10^5), 705 (2.53×10^5). m/z (HR-MALDI): calcd, 2819.8639 ($C_{160}H_{274}N_8O_{16}S_8$); found, 2819.8679 ($M^+$).

Acknowledgment. This work has been financially supported by the European Union (FP6-NAIMO integrated project NMP4-CT-2004-500355 and the FP6-STAG project), by FNRS (Grant 2.4613.07 for ULB), and by the Belgian Federal Science Policy Office (PAI FS2). B.T. is an FRIA research fellow. J.C. and S.S. are FNRS research fellows.

Supporting Information Available: Synthetic details and analytical data for **2a** and **4b**,**c**; computational details; powder X-ray diffraction data; electrochemical data; and MS data for the attempted synthesis of **1a** from **2a** (PDF). This information is available free of charge via the Internet at http://pubs.acs.org.